










Publication Year	2022
Acceptance in OA	2022-03-24T11:07:49Z
Title	7Be in the outburst of the ONe nova V6595 Sgr
Authors	MOLARO, Paolo, Izzo, L., D'ODORICO, Valentina, Aydi, E., Bonifacio, P., CESCUTTI, GABRIELE, Harvey, E. J., Hernanz, M., Selvelli, P., DELLA VALLE, Massimo
Publisher's version (DOI)	10.1093/mnras/stab3106
Handle	http://hdl.handle.net/20.500.12386/31857
Journal	MONTHLY NOTICES OF THE ROYAL ASTRONOMICAL SOCIETY
Volume	509

^7Be in the outburst of the ONe nova V6595 Sgr

P. Molaro ^{1,2}★, L. Izzo ³★, V. D’Odorico,¹ E. Aydi ⁴, P. Bonifacio ⁵, G. Cescutti ^{1,2,9}, E. J. Harvey ⁶, M. Hernanz ⁷, P. Selvelli¹ and M. della Valle⁸

¹INAF-Osservatorio Astronomico di Trieste, Via G.B. Tiepolo 11, I-34143 Trieste, Italy

²Institute of Fundamental Physics of the Universe, Via Beirut 2, Miramare, Trieste, Italy

³DARK, Niels Bohr Institute, University of Copenhagen, Jagtvej 128, 2200 Copenhagen, Denmark

⁴Center for Data Intensive and Time Domain Astronomy, Department of Physics and Astronomy, Michigan State University, East Lansing, MI 48824, USA

⁵GEPI, Observatoire de Paris, Université PSL, CNRS, Place Jules Janssen, 92195 Meudon, France

⁶Astrophysics Research Institute, Liverpool John Moores University, Liverpool, L3 5RF, UK

⁷Institute of Space Sciences (ICE, CSIC) and IEEC, Campus UAB, Camí de Can Magrans s/n, 08193 Cerdanyola del Valles (Barcelona), Spain

⁸Capodimonte Astronomical Observatory, INAF-Napoli, Salita Moiriello 16, 80131-Napoli, Italy

⁹INFN, Sezione di Trieste, Via A. Valerio 2, I-34127 Trieste, Italy

Accepted 2021 October 20. Received 2021 October 18; in original form 2021 August 9

ABSTRACT

We report on the search for the ^7Be II isotope in the outbursts of the classical nova V6595 Sgr by means of high-resolution Ultraviolet and Visual Echelle Spectrograph (UVES) observations taken at the European Southern Observatory’s Very Large Telescope in 2021 April, about two weeks after its discovery and under difficult circumstances due to the pandemic. Narrow absorption components with velocities at ~ -2620 and -2820 km s⁻¹, superposed on broader and shallow absorption, are observed in the outburst spectra for the ^7Be II $\lambda\lambda 313.0583, 313.1228$ nm doublet resonance lines, as well as in several other elements such as Ca II, Fe I, Mg I, Na I, H I and Li I. Using the Ca II K line as a reference element, we infer $N(^7\text{Be})/N(\text{H}) \approx 7.4 \times 10^{-6}$, or $\approx 9.8 \times 10^{-6}$ when the ^7Be decay is taken into account. The ^7Be abundance is about half of the value most frequently measured in novae. The possible presence of overionization in the layers where ^7Be II is detected is also discussed. Observations taken at the Telescopio Nazionale Galileo in La Palma 91 days after discovery showed prominent emission lines of oxygen and neon, which allow us to classify the nova as ONe type. Therefore, although ^7Be is expected to be higher in CO novae, it is found at comparable levels in both nova types.

Key words: nuclear reactions, nucleosynthesis, abundances – stars: abundances – stars: individual: V6595 Sgr – novae, cataclysmic variables – Galaxy: evolution.

1 INTRODUCTION

Classical novae (CNe) are recurring thermonuclear explosions in binary-star systems formed by a white dwarf (WD) accreting matter from a main-sequence or evolved companion (Bode & Evans 2012; Della Valle & Izzo 2020). The layer of accreted material grows in mass until the pressure at its bottom becomes sufficiently high ($> 2 \times 10^{19}$ dyne cm⁻²) for the beginning of nuclear ignition of the p–p chain. Because the bottom of the accreted layer is electron degenerate, nuclear burning increases the temperature without expansion that would inhibit further nuclear reactions. When the temperature becomes sufficiently high ($T > 10^7$ K), the energy source shifts to the CNO cycle and both temperature and energy release increase at a much faster rate. When pressure and temperature at the bottom of the accreted layer exceed the degeneracy values, thermonuclear reactions (TNRs) ignite, removing degeneracy and causing ejection of matter into the interstellar medium (Gallagher & Starrfield 1978). The subsequent expansion of the hot envelope at velocities of the order of 500–3000 km s⁻¹ is responsible for the initial brightness of

the nova, which can reach an absolute magnitude of $V \sim -9.5$ mag (Selvelli & Gilmozzi 2019).

Synthesis of lithium in novae explosions was first predicted in the 1970s (Arnould & Norgaard 1975; Starrfield et al. 1978). Lithium is created in the thermonuclear runaway via the reaction $^3\text{He}(\alpha, \gamma)^7\text{Be}$ with ^7Be decaying to ^7Li via electron capture (half-life 53.22 d). The production proceeds through the so-called Cameron–Fowler mechanism (Cameron 1955; Cameron & Fowler 1971) where ^7Be has to be transported to cooler zones than where it is formed, with a time-scale shorter than its electron capture time, and therefore preserved from destruction.

The suggestion, which dates back to the 1970s, was thwarted by the non-detection of ^7Li in a number of novae (Friedjung 1979). After decades of observational failures to detect the Li I 670.8 nm line, the parent nucleus ^7Be was detected in CNe (Tajitsu et al. 2015, 2016; Molaro et al. 2016; Izzo et al. 2018; Molaro et al. 2020; Arai et al. 2021), because of high-resolution spectrographs capable of reaching the atmospheric cut-off. Following these detections, a search in high dispersion spectra of historical novae in the archival database of the space-based *International Ultraviolet Explorer* (IUE) led to the identification of the ^7Be II resonance line in nova V838 Her, which had been overlooked (Selvelli, Molaro & Izzo 2018). The possible

* E-mail: paolo.molaro@inaf.it (PM); luca.izzo@gmail.com (LI)

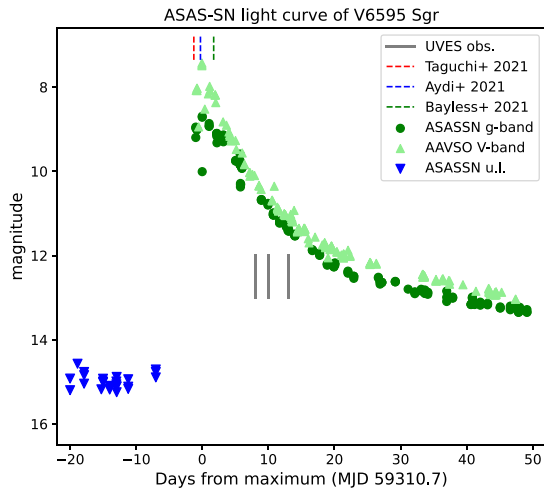


Figure 1. The ASAS-SN (Kochanek et al. 2017) g-band (green circles) and the American Association of Variable Star Observers (AAVSO; see <https://www.aavso.org>) V-band (light green triangles) light curves of V6595 Sgr. The blue triangles correspond to ASAS-SN upper limits. The black dashed lines mark the epochs of the VLT/UVES spectroscopic observations, presented in this work.

presence of the ⁷Li 670.8 nm resonance line in nova V1369 Cen (Izzo et al. 2015) was also reported. The detection of the short-lived ⁷Be in the spectra of novae shortly after outburst implies that this isotope is freshly created in the thermonuclear runaway processes of the nova event. ⁷Be decays with capture of an internal K-electron and ends in an ionized lithium, whose ground-state transitions are not observable in the optical range, thus explaining the general non-detection of neutral ⁷Li (Molaro et al. 2016). The decay of ⁷Be into an excited state of ⁷Li produces a high-energy line at 478 keV emitted during the de-excitation to the ground state of the fresh ⁷Li produced in the ⁷Be electron-capture (Clayton 1981; Gomez-Gomar et al. 1998). There have been several unsuccessful attempts to detect the line with gamma-ray satellites (Harris et al. 2001). The detection of the radioactive ⁷Be nuclei in the nova outburst reopened the possibility of detecting the 478 keV line with INTEGRAL for nearby novae. The distance should be lower than ≈ 0.5 kpc, though the horizon would depend on the amount of ⁷Be produced in the nova event (Jean et al. 2000; Siegert et al. 2018, 2021). We note that the detection of the 478 keV line from a nova with known distance will allow us to derive an accurate ⁷Be abundance.

The astrophysical origin of lithium represents a major open question in modern astrophysics (Fields 2011). The abundance of lithium observed in halo and metal-rich disc stars is much lower and higher, respectively, than the primordial value estimated from big bang nucleosynthesis once the baryonic density from the cosmic microwave background or deuterium abundance is adopted. This implies the existence of efficient lithium sinks and factories, which are both still unknown. For the latter, many astrophysical sources can actively produce lithium, such as AGB stars (Romano et al. 2001), red giants (Wallerstein & Sneden 1982), classical novae (Starrfield et al. 1978) or spallation processes (Davids, Laumer & Austin 1970). Early Galactic chemical evolution models of ⁷Li revealed that CNe show the required time-scales, but lithium nova yields were theoretically derived and not supported by observations at that time (D’Antona & Matteucci 1991; Romano et al. 1999, 2001). The recent measured yields imply massive ⁷Be ejecta with the final ⁷Li product at about four orders of magnitude above meteoritic abundance and novae are

very likely the major Li sources in the Galaxy (Molaro et al. 2016; Cescutti & Molaro 2019; Romano et al. 2021).

A major problem is that the measured abundances exceed what is foreseen by current nova nucleosynthesis models (Hernanz et al. 1996; José & Hernanz 1998), and it seems that ⁷Be is present in both fast and slow novae, with comparable abundances. Controversy arises about the maximum amount of ⁷Be II that can be produced in novae – see, for example, Denissenkov et al. (2021) and discussions in Starrfield et al. (2020) – but it remains well below what is derived from observations. Chugai & Kudryashov (2020) suggested that the presence of an overionization in the expanding shell of V5668 Sgr, where ⁷Be is observed, could reduce substantially the abundance of derived ⁷Be.

Following the recent detection of ⁷Be II in the outburst spectra of CNe, we started an observing programme at the European Southern Observatory (ESO) to target ⁷Be in novae that at maximum reach magnitude $V \leq 9$ mag. We report here on the observations of V6595 Sgr by means of the high-resolution Ultraviolet and Visual Echelle Spectrograph (UVES; Dekker et al. 2000) at the Very Large Telescope (VLT).

2 V6595 SGR

V6595 Sgr, originally reported as PNV J17581670–2914490,¹ was discovered on 2021 April 04.825 UT by Andrew Pearce at 8.4 mag. The nova was classified as a classical nova by Taguchi et al. (2021) and confirmed in follow-up spectra by Aydi et al. (2021). The All-Sky Automated Survey for Supernovae (ASAS-SN; Kochanek et al. 2017) light curve of V6595 Sgr is displayed in Fig. 1. The photometry shows that the nova is a very fast one, according to the historical classification by Gaposchkin (1957): it reached optical peak on 2021 April 06.2 (i.e. 1.4 d after its discovery), and faded by two magnitudes in 8.9 d. At the position reported in Ferreira, Saito & Minniti (2021), there is a single source in the *Gaia* EDR3 catalogue (Brown et al. 2021), namely GAIA 4062339124163281920. The *Gaia* magnitude is $g = 18.18$ mag, suggesting an amplitude of the outburst of $A = 9.49 \pm 0.40$ mag, with the uncertainty related to the different photometric systems used in the *Gaia* and ASAS-SN surveys.² No parallax is reported for this source in the *Gaia* Data Release 3 (DR3). Given the observed magnitude at peak of $V = 7.6$ mag (see Fig. 1), the reddening $R_V = 2.01$ mag, and the decay time of $t_2 = 8.9$ d, we can derive the absolute magnitude at the peak using the recent formulation of the maximum-magnitude and rate-decay (MMRD) relation given in Della Valle & Izzo (2020): we obtain $M_V = -9.08 \pm 0.22$ mag, resulting in a nova distance of $d_{\text{MMRD}} = 8.6 \pm 0.9$ kpc. The estimate from the MMRD relation is in good agreement with that estimated from the geometric distance ($M_V = -8.89 \pm 0.7$) and photogeometric distance ($M_V = -9.03 \pm 0.8$) (Bailer-Jones et al. 2021). The basic data for the V6595 Sgr are summarized in Table 1.

In early spectra of V6595 Sgr, Aydi et al. (2021) noted P-Cygni profiles and emission lines of low contrast relative to the continuum but with exceptional breadth. The Na I D interstellar absorption shows multiple components at velocities from 0 up to -215 km s⁻¹, suggesting high extinction towards the line of sight. From diffuse

¹<http://tamkin1.eps.harvard.edu/unconf/followups/J17581670-2914490.html>

²See, for example, the *Gaia* DR documentation release at https://gea.esac.esa.int/archive/documentation/GDR2/Data_processing/chap_cu5pho/sec_cu5pho_calibr/ssec_cu5pho_PhotTransf.html.

Table 1. V6595 Sgr: basic data.

Property	Value
Discovery	2021 April 04.825 UT
RA (J2000)	17 58 16.7
Dec. (J2000)	−29 14 49.0
Epoch max.	2021 April 06.2 UT
g_{\max}	8.69 mag
t_2	8.9 d
t_3	15.3 d
$E(B - V)$	0.65 mag
A	9.49 ± 0.40 mag
d_{MMRD}	8.6 ± 0.9 kpc

interstellar bands, Aydi et al. (2021) derived a colour excess $E(B - V) = 0.65$ mag, and $A_v = 2$ mag when assuming the standard Galactic extinction law $R_V = 3.1$. They also found this consistent with the reddening estimated from the Galactic reddening maps. Observations taken a few days later by Bayless et al. (2021) revealed strong emission lines, while the P-Cygni absorption mostly disappeared. They also noted that the emission lines were exceptionally broad with FWHM of 3500 km s^{-1} or greater. Fe II features were still present along with C I, N I and O I. The N I lines are unusually strong relative to C I, which, together with the presence of He I, indicates a rapid spectral evolution.

No X-ray emission has been detected by the *Swift*/X-ray telescope on 2021 April 5.86 (Sokolovsky et al. 2021). McCollum & Laine (2021) performed spectral energy distribution fitting of the available photometry for the progenitor object and with a set of model atmospheres found the best fit for $T_{\text{eff}} = 3750 \pm 150$ K, and $\log g = 3.5 \pm 0.3$. The value of A_V obtained from their best-fitting analysis is 1.26 ± 0.22 mag. In the following, we use this value to correct our spectral data set for Galactic extinction.

Three spectra for V6595 Sgr were obtained at the VLT/UVES following the peak brightness as soon as possible due to the critical pandemic circumstances. The UVES settings used were DIC1 346–564, with ranges 305–388 nm in the blue and 460–665 nm in the red, and DIC2 437–760 with ranges 360–480 nm in the blue, and 600–800 nm in the red. The journal of the observations for the nova is provided in Table 2. The nominal resolving power of the first two epochs was of for the blue arm and for the red arm. In the third observation, the slit was set to 1.2 arcsec and the pixels were binned two-by-two to cope with the nova fading, degrading by about half the previous resolution. Overlapping spectra were combined for each epoch to maximize the signal-to-noise ratio. In Fig. 2, we show the spectrum of V6595 Sgr obtained at VLT/UVES on 2021 April 16.

A spectrum of V6595 Sgr was also obtained on 2021 July 4, 91 d after discovery, by using the 3.6-m Telescopio Nazionale Galileo (TNG) equipped with the Device Optimized for the LOW RESolution (DOLORES) instrument in low-resolution spectroscopy

mode. Multiple exposures were obtained using the LR-B grism to optimize the signal-to-noise at wavelengths lower than 400 nm, and to avoid possible saturation of bright emission lines. The stacked spectrum covers the wavelength region between 330 and 800 nm and is shown in Fig. 3. The spectrum shows typical emission lines observed in the nebular phase of classical novae such as [O III], [O II] and [N II] (Della Valle & Izzo 2020). In particular, we identified bright forbidden [Ne III] and [Ne V] lines, with [Ne III] 386.9 nm being the most bright line in the spectrum (see Fig. 3). This suggests an overabundance of neon in the ejecta, which implies that V6595 is an ONe nova type (Williams et al. 1991). We also note the presence of relatively faint high-ionization iron forbidden lines, which are commonly observed during the super-soft phase of classical novae (Ness et al. 2007; Schwarz et al. 2011).

3 ^7Be DETECTION AND ABUNDANCE

Fig. 4 shows the three UVES spectra covering the beryllium region in the three epochs. The outburst spectra show absorption in a range of radial velocities spanning from -2000 to -3000 km s^{-1} . Figs 5 and 6 show the ^7Be spectra of April 16 and 19, respectively, along with the portions with the Ca II K, and H δ lines on a common velocity scale and normalized with a local continuum around the highlighted features. H δ is representative of the absorption seen in all members of the Balmer series. The Ca II H cannot be used as it is contaminated with H ϵ and, for this nova, its high velocity components are blended with the Galactic interstellar components of Ca II K. The appearance of the absorption is clear in all three elements. Superposed to a relatively shallow absorption, there are small but narrower structures at velocities of -2630 and -2815 km s^{-1} whose positions are marked on the figure. In all three spectra, there are hints of features that could be possibly ascribed to other lines of the ^7Be II doublet at a separation of 62 km s^{-1} . We preferred not to average the three spectra because, although taken rather closely in time, a small velocity drift of the components is always possible. The narrow features are hidden in the noise, but their presence in all three spectra makes us confident that they are real. We can also detect very weak lines of Cr II 312.870 nm and Fe II 313.536 nm at -2810 km s^{-1} . Because these weak lines are the strongest lines in the multiplets, they show that the contamination in the region is minimal and both Cr II and Fe II cannot be responsible for the observed absorption. It is also possible that the absorption could be in the form of a P-Cygni with ^7Be emission centred at rest wavelength and a large absorption shortwards. An emission in ^7Be II has been detected in the oxygen-poor nova V838 Her by Selvelli et al. (2018). However, here we focus on the absorption for which there is correspondence with other elements.

Relatively weak components make the detection more problematic but provide more reliable abundance estimation because saturation effects can be ignored. Shore & De Gennaro Aquino (2020) showed

Table 2. Journal of UVES observations and setting parameters.

Date	Time	B,R slit (arcsec)	Bin (pix)	346 nm (s)	437 nm (s)	564 nm (s)	760 nm (s)
2021/04/14	7:12	0.4, 0.3	1 x 1		60		60
2021/04/14	7:25	0.4, 0.3	1 x 1	300		60	
2021/04/16	8:04	1.2, 1.2	1 x 1		700		700
2021/04/16	8:44	1.2, 1.2	1 x 1	2310		2310	
2021/04/19	7:21	1.2, 1.2	2 x 2		900		900
2021/04/19	6:11	1.2, 1.2	2 x 2	3600		3600	

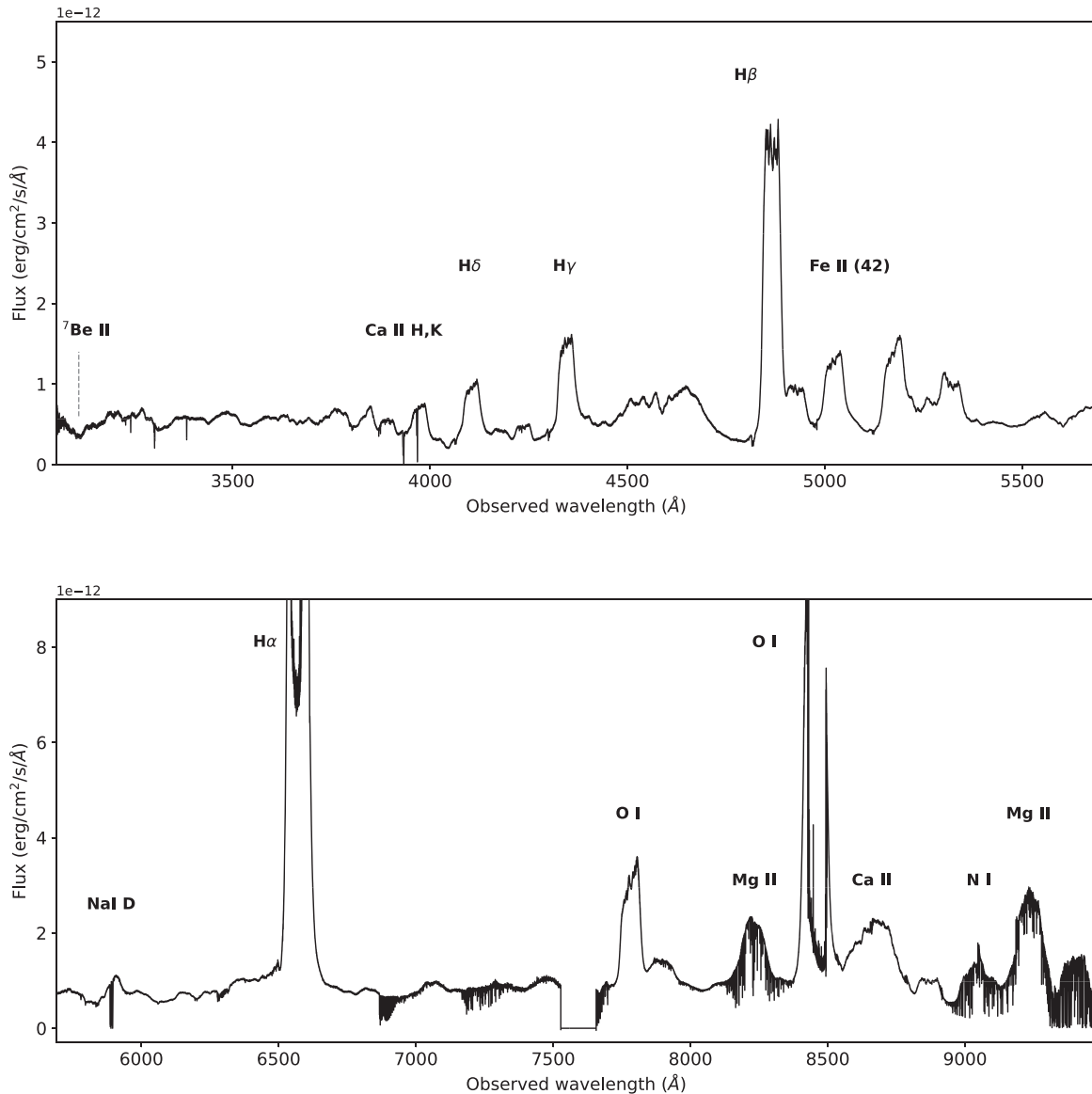


Figure 2. The spectrum of V6595 Sgr obtained at VLT/UVES on 2021 April 16. The upper panel shows the blue wavelength region (305–570 nm) while the red region (570–950 nm) is displayed in the lower panel. Some of the main visible features also used for the analysis presented in this work are marked in both panels. The $H\alpha$ and O I 844.6 nm features are saturated. The spectrum has been corrected for the interstellar extinction, using the value of $A_V = 1.26$ mag, as reported in Bayless, Rudy & Subasavage (2021).

that with high abundances the ^7Be II lines are strongly saturated and cannot be used. The ^7Be abundances are generally estimated taking Ca, which is not a nova product, as reference. Mg II, if available, could also be used for novae of the ONe Mg type (Casanova et al. 2016).

We do not detect doubly ionized ions, whose transitions are generally characterized by higher ionization potentials. However, we see the presence of neutral species such as Mg I 383.8, 383.2, 379.8 and 379.6 nm. Therefore, we assume that singly ionized ions of Ca II and ^7Be II are representing the main ionization stage in the expanding shell. This assumption has been criticized by Chugai & Kudryashov (2020) in the nova V5668 Sgr and will be addressed in detail in the next section.

As we cannot resolve the ^7Be II doublet for the shallow absorption, we consider the equivalent width (EW) of the sum of the ^7Be II

$\lambda 313.0583 + \lambda 313.1228$ doublet and compare it with the Ca II K line at 393.366 nm (Tajitsu et al. 2015; Molaro et al. 2016). We have

$$\frac{N(^7\text{Be II})}{N(\text{Ca II})} = 2.164 \times \frac{EW(^7\text{Be II, Doublet})}{EW(\text{Ca II, K})}, \quad (1)$$

where $\log(gf)$ of -0.178 and -0.479 for the ^7Be II doublet, and $+0.135$ for that of Ca II K line are adopted. The EW of the whole region spanned by the ^7Be II components as measured in the spectrum of April 16 is of 274 ± 15 mÅ, with the main uncertainty coming from the continuum placement. The EW of the Ca II 393.3-nm line is of 189 ± 8 mÅ, providing a ratio of $EW(^7\text{Be II})/EW(\text{Ca II}) \approx 1.45 \pm 0.15$. The same components as measured in the spectrum of April 19 are of $\approx 279 \pm 13$ mÅ and 165 ± 7 mÅ, providing a ratio of 1.69 ± 0.15 . We therefore

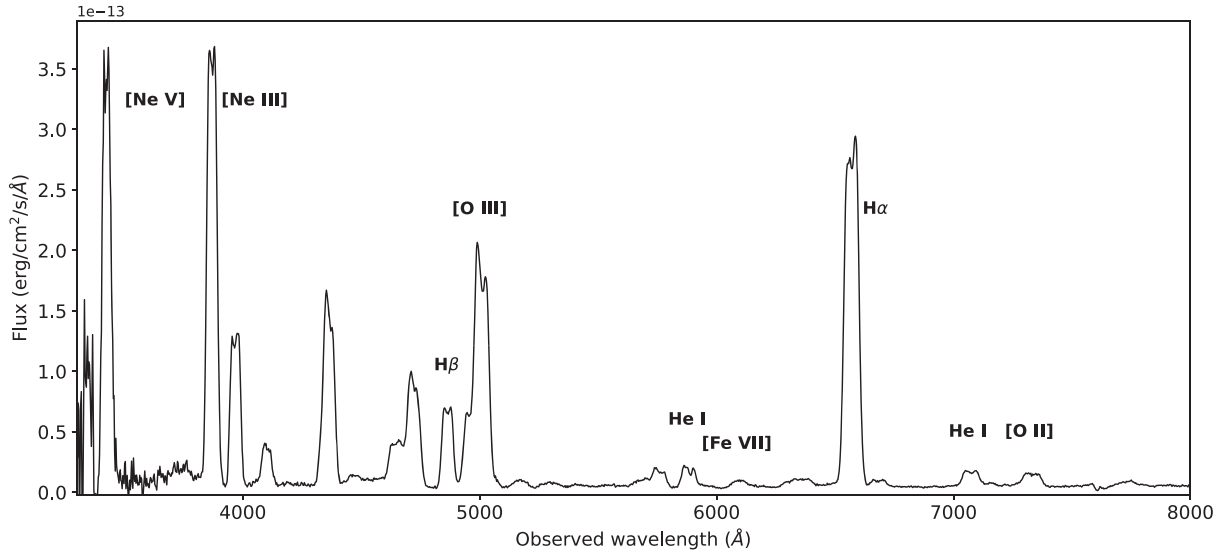


Figure 3. The TNG/DOLores spectrum of V6595 Sgr obtained 91 d after the nova discovery. The spectrum shows prominent emission lines of oxygen and neon, allowing us to classify the nova as a ONe type. The spectrum has been corrected for the interstellar extinction, using the colour excess value of $E(B - V) = 0.65$ mag (Bayless et al. 2021). Note that the flux level at wavelengths < 350 nm is not very accurate, given the low transmission efficiency of the camera.

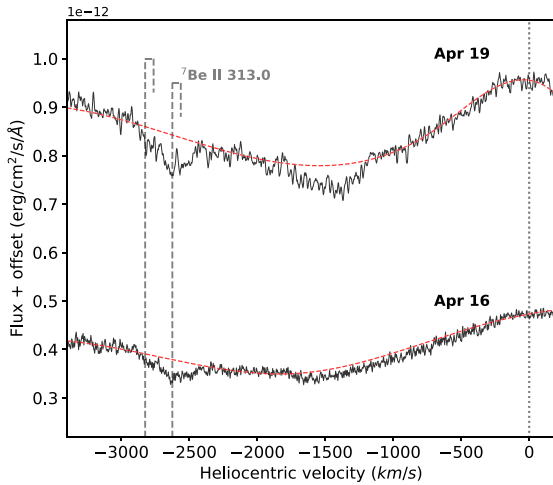


Figure 4. The ${}^7\text{Be}$ II 313-nm feature in two spectral epochs obtained with the VLT/UVES. The spectra are slightly smoothed to increase the signal-to-noise ratio. The dashed grey lines mark the position of the ${}^7\text{Be}$ II 313.0-nm doublet at the blueshifted heliocentric velocities of -2625 and -2810 km s^{-1} and the continuum is overlaid. The zero of the scale is set at ${}^7\text{Be}$ II $\lambda 313.0583$ nm.

adopt an average ratio of 1.57 ± 0.15 . Using equation (1), we obtain $N({}^7\text{Be II})/N(\text{Ca II}) = 3.4 \pm 0.15$. Because ${}^7\text{Be}$ is unstable with a half lifetime decay of 53.22 d, at the epoch of our measurement, 15 d from discovery, the abundance had reduced by a factor of 0.745. The solar abundance of calcium is $N(\text{Ca})/N(\text{H}) = 2.19 \pm 0.30 \times 10^{-6}$ (Lodders 2019). As a consequence, we obtain an abundance of $N({}^7\text{Be})/N(\text{H}) = 9.8 \times 10^{-6}$. Should calcium abundance be different from solar, the final $N({}^7\text{Be})/N(\text{H})$ would change accordingly. For instance, by extrapolating the Galactic metallicity gradient of Lemasle et al. (2018) towards the Galactic Centre, we should expect a metallicity of $[\text{Ca}/\text{H}] \approx +0.3$, which would imply $N({}^7\text{Be})/N(\text{H}) = 2.0 \times 10^{-5}$, namely a factor of 2 higher than is reported in Table 4.

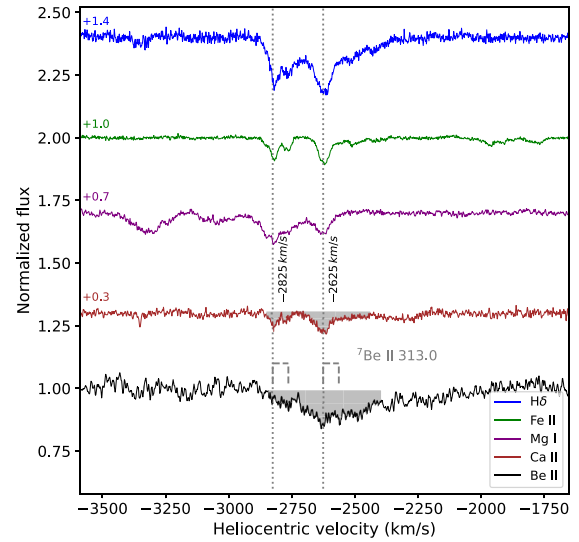


Figure 5. Normalized spectrum of April 16 in the regions of ${}^7\text{Be}$ II, Ca II K, Mg I 383.829 nm, Fe II 516.903 nm and H δ lines from bottom to top, respectively. The normalization has been performed by using the adjacent regions around the absorption. The narrow absorption features are marked with a dotted line while the shadowed area shows the shallow absorption.

3.1 Lithium

Fig. 7 shows the spectrum of April 16 in the region of ${}^7\text{Li}$ I 670.8 nm, together with the D2 line of Na I 589.0 nm and Ca I 422.6 nm. Absorptions are detected corresponding to the D2 and D1 lines with expansion velocities of -2625 and -2825 km s^{-1} but not corresponding to the Ca I and Li I lines. The same is found for the spectra of the other two epochs of April 14 and 19. Thus, there is no evidence of the resonance ${}^7\text{Li}$ I doublet at 670.8 nm in the spectra of V6596 Sgr as in most of the novae. So far, ${}^7\text{Li}$ I has been detected only in V1369 (Izzo et al. 2015) and, as a trace element, in a very early epoch of V906 Car (Molaro et al. 2020). The detection in

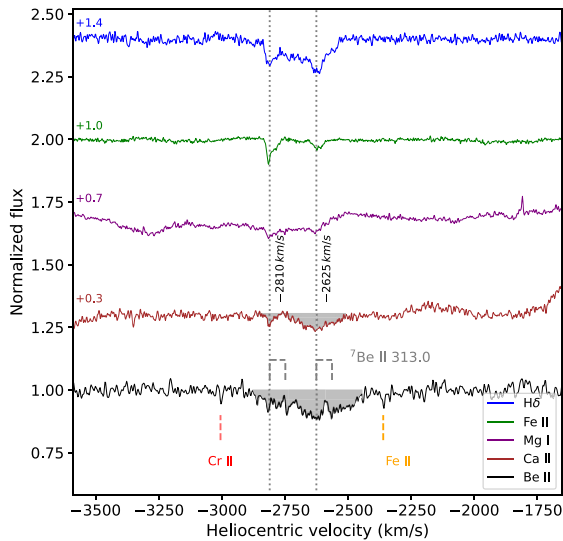


Figure 6. As in the previous figure but for the spectrum of April 19. Note that in this spectrum the faint and sharp lines for the -2810 km s^{-1} components of Cr II 312.870 nm and Fe II 313.536 nm can be identified in the spectrum.

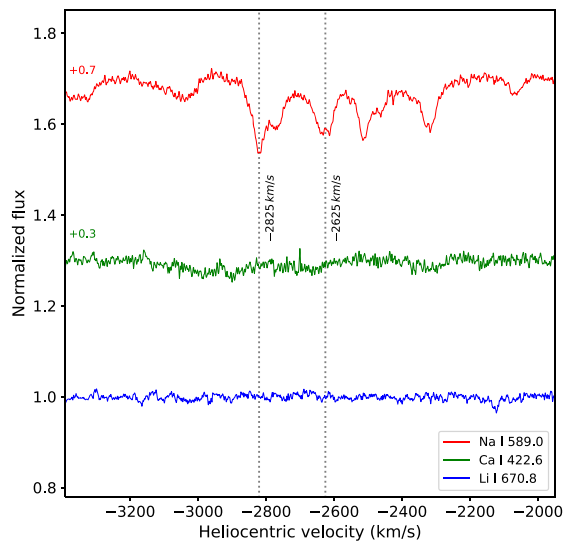


Figure 7. Spectra of April 16 in the regions of Na I 589.0 nm, Ca I 422.6 nm and ⁷Li I 670.8 nm. While blueshifted expanding absorptions are clearly detected for the Na I 589.0-nm line, there is no evidence of Ca I and ⁷Li I at the same expanding velocities. The absorptions of the D1 line are also visible redwards of the D2 line.

V1369 was determined on days 7 and 13 when only a small amount of ⁷Be had decayed into ⁷Li, which implies that the TNR started much earlier than the explosion (Izzo et al. 2015). A claim for a Li detection was made by Della Valle et al. (2002) in V382 Vel, but Shore et al. (2003) suggested that the feature could be neutral nitrogen. The general absence of neutral ⁷Li on a time-scale longer than the ⁷Be decay can be explained if ⁷Be decays through the capture of an internal K-electron. In this case, the end product is an ionized lithium with transition lines in the X-ray (Molaro et al. 2016).

4 DISCUSSION

4.1 Overionization?

The Be II abundances measured in the novae where it has been detected so far are high (see Table 4) and, in particular, are higher than the nova models predict. Recent reappraisal of the theoretical ⁷Be maximum that can be synthesized in novae is of $X(^7\text{Be})/X(\text{H}) \approx 2 \times 10^{-5}$ as mass fraction, or $N(^7\text{Be})/N(\text{H}) \approx 3 \times 10^{-6}$ in atomic fraction, for CO and relatively massive white dwarfs (Starrfield et al. 2020; Denissenkov et al. 2021; Chugai & Kudryashov 2020). ⁷Be abundances are generally derived assuming ⁷Be II and Ca II are both in their dominant ionization stage. Chugai & Kudryashov (2020) suggested that the disagreement between theoretical predictions and observations could be resolved if significant overionization is present in the expanding components. As the ionization potential of Be II and Ca II is 18.21 and 11.87 eV, respectively, the radiation from a hot photosphere could overionize Ca II and reduce the ⁷Be abundance derived from observations.

In nova V838 Her, Selvelli et al. (2018) obtained the ⁷Be abundance by using Mg II as a reference element. Mg has a second ionization potential of 15 eV, which is closer to Be II than Ca II, and the two ions should behave similarly. They obtained $N(^7\text{Be})/N(\text{H}) \approx 2 \times 10^{-5}$, a value that is similar to the value measured in the other nova where Ca II was used (as listed in Table 4). Selvelli et al. (2018) also derived consistent abundances by using He I and H I emission lines. This consistency would not be expected in the presence of significant overionization.

Chugai & Kudryashov (2020) analyse in detail the case of nova V5668 Sgr studied by Molaro et al. (2016) and Tajitsu et al. (2016), and concentrate on the component at velocity -1175 km s^{-1} shown at day 58. No doubly ionized states of Fe-peak elements with second ionization potentials intermediate to those of ⁷Be (18.21 eV) and Ca II (11.87 eV) are observed corresponding to this high-velocity component of nova V5668 Sgr (Molaro et al. 2016; Tajitsu et al. 2016). This was one major justification used in Tajitsu et al. (2015) and Molaro et al. (2016) to consider ⁷Be and Ca II in the main ionization state in V5668. However, hints of the neutral species of Ca I and Na I are reported (see fig. 7 of Molaro et al. 2016). For any combination of physical parameters, it is not possible to have Ca III and Ca I in the same slab of material.

Chugai & Kudryashov (2020) argue for the presence of partial covering and of multiple components. However, they obtain a Be II/Ca II ratio of 36.6, which is close to the value of 31.9 derived by Molaro et al. (2016) for this component. We note that the measured Be II/Ca II = 31.9 implies a $X(^7\text{Be})/X(\text{H})$ mass fraction of 1.2×10^{-3} and not of 9×10^{-5} as reported by Chugai & Kudryashov (2020). Thus, a correction of two orders of magnitude is required to reconcile these abundances with the theoretical ⁷Be production. The pseudo-photosphere of the nova in the model of Chugai & Kudryashov (2020) is approximated with a blackbody with a temperature of $\approx 15000 \text{ K}$, and a radius of 10^{12} cm , for a total luminosity of $\sim 3.6 \times 10^{37} \text{ erg s}^{-1}$. The high-velocity component showing ⁷Be II is located at a distance of $6 \times 10^{14} \text{ cm}$, which is the distance reached after 58 d when moving with a velocity of $v_{\text{exp}} = -1175 \text{ km s}^{-1}$, and it has a thickness which is 10 per cent of its radius. Chugai & Kudryashov (2020) assume a mass of $10^{-5} M_{\odot}$ for this component, which with the assumed volume results in a gas density of $\log(n_{\text{H}}) = \log(n_{\text{e}}) = 7.6 \text{ cm}^{-3}$. This shell feels the radiation coming from the nova pseudo-photosphere and Chugai & Kudryashov (2020) estimate Ca III/Ca II ≈ 10 in the expanding shell with velocity of -1175 km s^{-1} . This means that the Ca II is not the main stage and

Table 3. Mean ionization for relevant elements obtained with CLOUDY for different conditions of the photosphere and for the expanding component. We give the logarithmic fraction of an ionization stage over the total. Model A is the model considered in Chugai & Kudryashov (2020), with the photosphere of a blackbody with a temperature of $T = 15\,000$ K, radius $r = 10^{12}$ cm and total luminosity of 38.3. The expanding shell with ${}^7\text{Be}$ has a gas density of $\log(n_{\text{H}}) = \log(n_{\text{H}}) = 7.6$ cm $^{-3}$. Model B is as Model A but with a gas density in the clump of $\log(n_{\text{H}}) = \log(n_{\text{H}}) = 10$ cm $^{-3}$. Model C is intermediate with a blackbody temperature of $T = 10\,000$ K and a gas density in the clump of $\log(n_{\text{H}}) = 9$ cm $^{-3}$.

El Ion	Model A			Model B			Model C		
	I	II	III	I	II	III	I	II	III
H	-0.71	-0.09		-0.03	-1.15		-0.02	-1.40	
He	-0.01	-1.81		0.00	-5.18		0.00	-9.01	
Li	-5.21	0.00		-3.83	0.00		-4.68	0.00	
Be	-4.22	-0.28	-0.32	-2.82	0.00	-4.55	-3.30	0.00	-762
Na	-3.82	0.00	-12.14	-2.54	0.00	-12.50	-3.23	0.00	-19.20
Mg	-4.40	-0.31	-0.30	-2.77	0.00	-2.85	-3.45	0.00	-3.11
Ca	-7.82	-2.24	0.00	-4.42	-0.23	-0.39	-5.05	-0.01	-1.55
Cr	-5.79	-0.38	-0.23	-4.14	0.00	-2.41	-4.56	0.00	-3.25
Fe	-5.45	-0.35	-0.26	-4.27	0.00	-2.84	-4.47	0.00	-3.64

the ${}^7\text{Be}$ abundance previously estimated should be decreased by one order of magnitude.

We have used version 17.03 of the photoionization code CLOUDY (Ferland et al. 2017) to probe photoionization conditions within the absorption component. In a first model, Model A, we adopted the same model as Chugai & Kudryashov (2020) with a temperature of the nova photosphere of 15 000 K. The results, reported in Table 3, show that Ca II is indeed much more ionized than Be II and even for a larger fraction than that estimated by Chugai & Kudryashov (2020). However, the question is whether the model provides a realistic description of nova photosphere and of the expanding shell where ${}^7\text{Be}$ is observed. The gas density in the expanding shell is probably higher than assumed. Harvey et al. (2018) at day 141 measure an electron density of $\log(n_{\text{H}}) = 9$ cm $^{-3}$, which is higher than the 7.6 assumed by Chugai & Kudryashov (2020) 80 d earlier. Moreover, the formation of dust requires shielding from the WD’s radiation, which is possible if the gas density is greater than $\log(n_{\text{H}}) = 9$ – 10 cm $^{-3}$ (Gehrz & Ney 1987). Gehrz et al. (2018) found evidence that dust condensation in V5668 Sgr commenced 82 d after outburst and estimated an envelope temperature of 1090 K. Muztaba, Malasan & Arai (2020) modelled with CLOUDY the spectrum of V5668 Sgr on 2015 June 12, or day 89, with the nova in the dust production phase and matching fairly well the emission spectrum with a temperature for the nova envelope of 6509 K. At day 107, Banerjee et al. 2016 modelled the CO emission line with a temperature of 4000 ± 300 K.

We thus constructed a new model, Model B, with a temperature of $T = 15\,000$ K for the nova envelope but with a gas density in the clump of $\log(N_{\text{H}}) = 10$ cm $^{-3}$. The higher density is obtained by reducing the thickness of the expanding shell and the filling factor. We have also constructed an intermediate model, Model C, with a blackbody temperature of 10 000 K and a gas density of $\log(n_{\text{H}}) = 9$ cm $^{-3}$. The mean ionizations for the relevant elements are listed in Table 3. In both Models B and C, the Ca II and Be II are found in their main ionization stages. Fig. 8 shows the relative ionization fractions for ${}^7\text{Be}$ and Ca II for the two blackbody temperatures for a wider range of gas densities. Thus, overionization is possible only for very low gas densities and a hot pseudo-photosphere.

We emphasize that measured ${}^7\text{Be}$ abundances in V5668 Sgr, obtained in components with different expanding velocities and also at different epochs, show consistency (Molaro et al. 2016). For instance, at day 58, the component with $v_{\text{exp}} = -1175$ km s $^{-1}$ shows $\text{Be II}/\text{Ca II} = 31.9$ while the component expanding with a velocity of -1500 km s $^{-1}$ at day 82 shows $\text{Be II}/\text{Ca II} = 17.7$. Interestingly, these two ratios become 69 and 53, respectively, when the ${}^7\text{Be}$

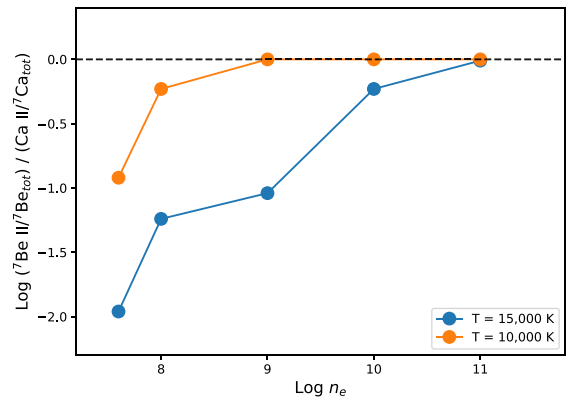


Figure 8. Relative mean ionization of ${}^7\text{Be II}$ and Ca II, $\log(\text{Be II}/\text{Be II})/(\text{Ca II}/\text{Ca})$, for different values of gas densities and for two temperatures of the pseudo-photosphere.

decaying factors are considered. We consider it unlikely that the physical conditions producing overionization could remain similar in two shells expanding with different velocities and measured in two epochs separated by a time interval of 24 d.

A satisfactory physical model is presently not available because of the poor understanding of the nova ejecta. However, for the arguments provided here, we consider it unlikely that the disagreement between theoretical predictions using nova models and ${}^7\text{Be}$ abundances derived from observations could be ascribed to the presence of overionization in the expanding shells.

4.2 ${}^7\text{Be}$ nova yields

The presence of ${}^7\text{Be}$ in a high-velocity component in the outburst spectra of V6595 Sgr adds another object to the small sample of novae where ${}^7\text{Be}$ has been searched and found. The $A({}^7\text{Be}) = \log N({}^7\text{Be})/N(\text{H I}) + 12$ abundances of these novae are listed in Table 4 and shown in Fig. 9. So far, ${}^7\text{Be}$ has been found in all the novae where it has been searched for except for V612 Sct, which has been suggested could be peculiar (Mason et al. 2020). By means of a low-resolution spectrum of V6595 Sgr taken 91 d after the discovery, which shows prominent lines of forbidden Ne III and [Ne v] lines, we classified the nova as ONe type (Williams et al. 1991). V6595 Sgr is, together with V407 Lup, a second nova of ONe type where ${}^7\text{Be}$ has been detected. Nova V838 Her is a third but with some

Table 4. $A(^7\text{Be})$ abundances for the novae with narrow absorption components. The literature values are computed from the original $W(^7\text{Be II, doublet})/W(\text{Ca II K})$ by taking the same ID recommended solar $A(\text{Ca}) = 6.34 \pm 0.06$ from Lodders (2019) but V838 Her where magnesium was used. $N(^7\text{Be})/N(\text{H})_c$ are the values corrected for the ⁷Be decay with a mean life of 76.8 d. References are: (1) Tajitsu et al. (2015) – note that they did not correct for the ⁷Be decay; (2) Molaro et al. (2016); (3) Izzo et al. (2018); (4) Tajitsu et al. (2016); (5) Selvelli et al. (2018) – the measurement from Mg II absorption is reported; (6) Molaro et al. (2020) – V612 Sct could be a peculiar object (Mason et al. 2020); (7) Arai et al. (2021); (8) Izzo et al. (2015) – the ⁷Li abundance is measured from ⁷Li I 670.8 nm and ionization is estimated with the Na I and K I lines, and the latter is labelled with an asterisk; (9) this paper.

Nova	Type	d	Comp. (km s ⁻¹)	$A(^7\text{Be})$	$A(^7\text{Be})_c$	Ref
V339 Del	CO	47	-1103	6.92	7.20	1,4
V339 Del	CO	47	-1268	7.11	7.38	1,4
V5668 Sgr	CO	58	-1175	7.84	8.17	2
V5668 Sgr	CO	82	-1500	7.58	8.04	2
V2944 Oph	CO	80	-645	6.72	7.18	4
V407 Lup	ONe	8	-2030	7.69	7.73	3
V838 Her	ONe?	3	-2500	7.66	7.68	5
V612 Sct	?			-	-	6
V357 Mus	CO?	35	≈ -1000	6.96	7.18	6
FM Cir	CO?				:	6
V906 Car	CO?	80	≈ -600	6.86	7.30	6
V5669 Sgr	CO	28	≈ -1000	6.34	6.51	7
V5669 Sgr	CO	28	≈ -2000	6.61	6.77	7
V6595 Sgr	ONe	15	-2700	6.87	6.99	9
V1369 Cen	CO	7	-550	5.00	5.04	8
V1369 Cen	CO	13	-560	5.30	5.38	8
V1369 Cen*	CO	7	-550	4.70	4.78	8
V1369 Cen*	CO	13	-560	4.78	4.85	8

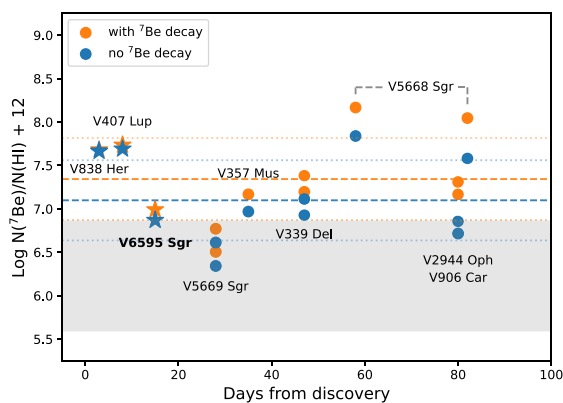


Figure 9. ⁷Be abundances as a function of the day of observation with, in orange, and without correction for the ⁷Be decay, in blue. The two ONe novae are shown with a star while the CO novae with a circle. The dashed lines mark the average value for both estimates. $\log N(^7\text{Be})/N(\text{HI}) + 12 = 7.34 \pm 0.47$ when ⁷Be decay is taken into account, and $\log N(^7\text{Be})/N(\text{HI}) + 12 = 7.10 \pm 0.46$, when it is not. The grey band shows the range of ⁷Be yields for WD of different masses according to Starrfield et al. (2020). With this scale the meteoritic abundance is of $A(^7\text{Li}) = 3.3$. The novae show a mean overabundance of four orders of magnitude (Lodders 2019).

peculiarities being deficient in oxygen (Matheson, Filippenko & Ho 1993). The ONe novae show different ⁷Be abundances, with V407 Lup being about six times higher than V6595 Sgr. The synthesis of ⁷Be is believed to occur via ³He(α , γ)⁷Be in both types of CO and ONe novae but is expected to be one order of magnitude higher in CO

novae because of the different time-scales of the TNR in the two types of novae (José & Hernanz 1998). The ONe show ⁷Be abundances that overlap those of the CO novae. While V6595 Sgr shows among the lowest abundance of the sample, V407 Lup is slightly higher and V838 Her is aligned with the mean value of the CO novae. This supports the evidence that the ⁷Be abundance is uncorrelated from the nova type. We note that in the ONe type the ⁷Be detection was made in the early phases when the nova pseudo-photosphere is hotter. Thus, overionization is more likely to occur in fast novae, and the ⁷Be of ONe could be lower than the CO type as expected from the TNR theory.

The nine ⁷Be measurements show a scatter that exceeds the observational errors and is likely real. The mean value is of $A(^7\text{Be}) = 7.34 \pm 0.47$ when the ⁷Be decay is taken into account, which is about four orders of magnitude over the meteoritic value (Lodders 2019). The role of novae as ⁷Li producers has been considered in a framework of a detailed model of the chemical evolution of the Milky Way (Cescutti & Molaro 2019; Romano et al. 2021). Cescutti & Molaro (2019) showed that novae account well for the observed increase of Li abundance with metallicity in the Galactic thin disc and also for the relative flatness observed in the thick disc. In fact, the thick disc evolves on a time-scale that is shorter than the typical time-scale for the production of substantial ⁷Li by novae. Cescutti & Molaro (2019) left the nova yields as a free parameter and found that in order to match the ⁷Li behaviour with metallicity and the present abundance, a ⁷Li production of $3 \times 10^{-9} M_{\odot}$ per nova event is required. This is consistent with the measured mean yields of ⁷Li/H of 1.5×10^{-4} in mass, and an average ejecta of $3 \times 10^{-5} M_{\odot}$. A constant nova rate of $\approx 20 \text{ yr}^{-1}$ during the Galactic life with these yields is able to synthesize $\approx 600 M_{\odot}$, i.e. about 60 per cent of the total ⁷Li estimated for the whole Galaxy, with the rest shared by big bang, $\approx 250 M_{\odot}$, and Galactic spallation nucleosynthesis, $\approx 100 M_{\odot}$.

Molaro et al. (2020) suggested that a higher ³He in the donor star could result in a higher ⁷Be as it is produced through the ³He(α , γ)⁷Be channel. Denissenkov et al. (2021) showed that an increased abundance of ³He in the accreted material leads to a decrease of the peak temperature, and therefore a reduced production of ⁷Be. They suggested instead that an enhanced abundance of ⁴He could favour ⁷Be production. However, McCollum & Laine (2021) found that the progenitor object of V6595 Sgr is a cool subgiant with $T_{\text{eff}} = 3750 \pm 150 \text{ K}$, and $\log g = 3.5 \pm 0.3$, which is unlikely to be enriched in either ³He or ⁴He.

Evidence of absorption components has always been observed in novae, in both hydrogen and metal lines. These absorptions show relatively narrow features, and are called transient heavy element absorptions (THEA) by Williams et al. (2008). Generally, these are the result of neutral and low-ionization transitions of elements that are detected during the optically thick phases of classical novae. They exhibit only a single, low-velocity absorption component, suggesting that they are located in a toroidal ejecta surrounding the nova progenitor. These lines are visible only for a limited time interval, generally a few weeks after the nova discovery, before disappearing and leaving a spectrum dominated by Balmer lines, Fe II, elements synthesized in the TNR and, at later times when the ionization state increases, by helium. From a study of their evolution in V906 Car, Aydi et al. (2020) argued that they might be located in the slow ejecta component. The detection of high-energy emission in gamma-rays combined with the evidence of delayed components in the optical has challenged the nova phenomenology. Aydi et al. (2020) suggested that the nova outburst consists of early dense toroidal ejecta moving outward with relatively slow ($< 1000 \text{ km s}^{-1}$)

velocities, which produce the first bright optical peak in the emission. Later, a faster wind-like component with larger velocities will catch up with the earlier slower ejecta, thus producing shocks that will be observed at high energies. They concluded that THEA could be pre-existing material surrounding the system.

The ^7Be absorption line observed in V6595 Sgr is expanding at almost 3000 km s^{-1} , which is the highest recorded velocity for ^7Be in all novae. However, in V2944 Oph, the velocity of the ^7Be absorption is -645 km s^{-1} . V5668 Sgr also shows $^7\text{Be II}$ lines in a component at -730 km s^{-1} and also in components with velocities up to 2200 km s^{-1} . By taking these figures at face value, ^7Be is found in both high- or low-velocity components of nova outbursts. This shows that TNR products are also present in the slower material.

Denissenkov et al. (2021) noted that the conditions after 71 min at the end of the nova trajectory imply a small occupation probability for K-shell electrons, suggesting that ^7Be is fully ionized and practically stable. They computed the effective lifetime to be of the order of $5 \times 10^6 \text{ d}$. Fig. 9 shows the ^7Be abundances both with and without the decay correction. When ^7Be decay is not taken into account, the average value is $\log[N(^7\text{Be})/N(\text{H I})] + 12 = 7.10 \pm 0.46$. The two sets of measurements show a similar scatter, which exceeds the observational errors and is likely intrinsic. The values without correction are significantly smaller and closer to the maximum theoretical values. With this scenario, the distance between observed abundances and theoretical models is much reduced. V5668 Sgr is the only nova where two independent measures of the ^7Be abundance have been taken in two different epochs, at 58 and 82 d after maximum, respectively. The abundances differ by a factor of 1.8 when the decay is not taken into account, but by only 30 per cent (i.e. within the measurement errors) when the decay is considered. Thus, in this case it seems that correction for the decay provides a more plausible behaviour. Moreover, we note that the mere presence of the $^7\text{Be II}$ lines in the outburst nova spectra is not consistent with ^7Be remaining fully ionized for such a long time.

5 SUMMARY

High-resolution observations of the classical nova V6595 Sgr taken with the UVES after few days from explosion have been analysed to search for the presence of the $^7\text{Be II}$ doublet lines. The main results are the following.

(i) The spectra showed the presence of a shallow absorption feature due to the $^7\text{Be II}$ doublet lines spanning very high velocities from -2600 to -2900 km s^{-1} . Superposed there are narrow absorption components with velocities at ~ -2620 and -2820 km s^{-1} . The absorptions are also seen in several other elements such as Mg I, Na I, Ca II, Fe II and H I. The ^7Be detection in very high velocity ejecta components shows that both high- and low-velocity components contain material processed in the thermonuclear runaway.

(ii) Using the Ca II K line as a reference element, we infer $X(^7\text{Be})/X(\text{H}) \approx 7.4 \times 10^{-6}$, or $\approx 9.8 \times 10^{-6}$ when the ^7Be decay is taken into account. The ^7Be abundance is about half of the value most frequently measured in novae.

(iii) Observations 91 d after discovery showed prominent emission lines of neon and oxygen, which allowed us to classify the nova as ONe type. ^7Be seems to be produced in both types at comparable levels.

(iv) The possible presence of overionization suggested by Chugai & Kudryashov (2020) in nova V5668 Sgr is discussed. The model adopted by Chugai & Kudryashov (2020) does indeed produce overionization in the observed layer, but it fails to reproduce

other observables and does not reproduce the physical conditions of the material where the ^7Be is observed. We therefore conclude that significant overionization effects are unlikely to occur. On the other hand, overionization could be present for the fast ONe novae resulting into a ^7Be abundance lower than CO novae, in better agreement with the theoretical expectations.

(v) The suggestion by Denissenkov et al. (2021) that ^7Be remains fully ionized and stable for a considerable time after the explosion is also discussed and found not to be consistent with the $^7\text{Be II}$ observations and their time variation.

ACKNOWLEDGEMENTS

Based on data from Paranal Observatory, ESO, Chile. The staff at the ESO is warmly acknowledged for the execution of these observations during the pandemic lockdown. An anonymous referee is warmly thanked for many useful suggestions. Based on observations made with the Italian Telescopio Nazionale Galileo (TNG) operated on the island of La Palma by the Fundación Galileo Galilei of the INAF (Istituto Nazionale di Astrofisica) at the Spanish Observatorio del Roque de los Muchachos of the Instituto de Astrofísica de Canarias. LI was supported by two grants from VILLUM FONDEN (project number 16599 and 25501). M. H. acknowledges support from grant PID2019-108709GB-I00 from MICINN (Spain). M. LI warmly thanks Ernesto Guido for the technical support and important discussions during the planning of the observations.

DATA AVAILABILITY

Based on data from the UVES at Unit 2 of the VLT at the Paranal Observatory, ESO, Chile. The observations have been taken under a Target opportunity Programme 105.20B6.001 (PI: P. Molaro). ESO data are available worldwide and can be requested after the proprietary period of one year by the astronomical community through the link <http://archive.eso.org/cms/eso-data.html>. Before this they will also be shared on reasonable request to the corresponding author.

REFERENCES

- Arai A., Tajitsu A., Kawakita H., Shinnaka Y., 2021, *ApJ*, 916, 44
 Arnould M., Norgaard H., 1975, *A&A*, 42, 55
 Aydi E. et al., 2020, *ApJ*, 905, 62
 Aydi E. et al., 2021, The Astronomer's Telegram, 14533, 1
 Bailer-Jones C. A. L., Rybizki J., Fouesneau M., Demleitner M., Andrae R., 2021, *AJ*, 161, 147
 Banerjee D. P. K., Srivastava M. K., Ashok N. M., Venkataraman V., 2016, *MNRAS*, 455, L109
 Bayless A. J., Rudy R. J., Subasavage J. P., 2021, The Astronomer's Telegram, 14553, 1
 Bode M. F., Evans A., 2012, *Classical Novae*. Cambridge Univ. Press, Cambridge
 Brown A. G. A. Gaia Collaboration et al. (Gaia Collaboration), 2021, *A&A*, 649, A1
 Cameron A. G. W., 1955, *ApJ*, 121, 144
 Cameron A. G. W., Fowler W. A., 1971, *ApJ*, 164, 111
 Casanova J., José J., García-Berro E., Shore S. N., 2016, *A&A*, 595, A28
 Cescutti G., Molaro P., 2019, *MNRAS*, 482, 4372
 Chugai N. N., Kudryashov A. D., 2020, preprint ([arXiv:2007.07044](https://arxiv.org/abs/2007.07044))
 Clayton D. D., 1981, *ApJ*, 244, L97
 D'Antona F., Matteucci F., 1991, *A&A*, 248, 62
 Davids C. N., Laumer H., Austin S. M., 1970, *Phys. Rev. C*, 1, 270
 Dekker H., D'Odorico S., Kaufer A., Delabre B., Kotzlwski H., 2000, *Proc. SPIE*, 4008, 534
 Della Valle M., Izzo L., 2020, *A&AR*, 28, 3

- Della Valle M., Pasquini L., Daou D., Williams R. E., 2002, *A&A*, 390, 155
- Denissenkov P. A., Ruiz C., Upadhyayula S., Herwig F., 2021, *MNRAS*, 501, L33
- Ferland G. J. et al., 2017, *Rev. Mex. Astron. Astrofis.*, 53, 385
- Ferreira T. S., Saito R. K., Minniti D., 2021, *The Astronomer's Telegram*, 14625, 1
- Fields B. D., 2011, *Annual Review of Nuclear and Particle Science*, 61, 47
- Friedjung M., 1979, *A&A*, 77, 357
- Gallagher J. S., Starrfield S., 1978, *ARA&A*, 16, 171
- Gaposchkin C. H. P., 1957, *The Galactic Novae*. North-Holland, Amsterdam
- Gehrz R. D., Ney E. P., 1987, *Proceedings of the National Academy of Science*, 84, 6961
- Gehrz R. D. et al., 2018, *ApJ*, 858, 78
- Gomez-Gomar J., Hernanz M., Jose J., Isern J., 1998, *MNRAS*, 296, 913
- Harris M. J., Teegarden B. J., Weidenspointner G., Palmer D. M., Cline T. L., Gehrels N., Ramaty R., 2001, *ApJ*, 563, 950
- Harvey E. J., Redman M. P., Darnley M. J., Williams S. C., Berdyugin A., Piroola V. E., Fitzgerald K. P., O'Connor E. G. P., 2018, *A&A*, 611, A3
- Hernanz M., Jose J., Coc A., Isern J., 1996, *ApJ*, 465, L27
- Izzo L. et al., 2015, *ApJ*, 808, L14
- Izzo L. et al., 2018, *MNRAS*, 478, 1601
- Jean P., Hernanz M., Gómez-Gomar J., José J., 2000, *MNRAS*, 319, 350
- José J., Hernanz M., 1998, *ApJ*, 494, 680
- Kochanek C. S. et al., 2017, *PASP*, 129, 104502
- Lemasle B. et al., 2018, *A&A*, 618, A160
- Lodders K., 2019, preprint ([arXiv:1912.00844](https://arxiv.org/abs/1912.00844))
- Mason E., Shore S. N., Kuin P., Bohlsen T., 2020, *A&A*, 635, A115
- Matheson T., Filippenko A. V., Ho L. C., 1993, *ApJ*, 418, L29
- McCullum B., Laine S., 2021, *The Astronomer's Telegram*, 14655, 1
- Molaro P., Izzo L., Mason E., Bonifacio P., Della Valle M., 2016, *MNRAS*, 463, L117
- Molaro P., Izzo L., Bonifacio P., Hernanz M., Selvelli P., della Valle M., 2020, *MNRAS*, 492, 4975
- Muztaba R., Malasan H. L., Arai A., 2020, in *IOP Conf. Series: Earth and Environmental Science*, Vol. 537. IOP Publishing, Bristol, p. 012004 (doi:10.1088/1755-1315/537/1/012004)
- Ness J. U. et al., 2007, *ApJ*, 665, 1334
- Romano D., Matteucci F., Molaro P., Bonifacio P., 1999, *A&A*, 352, 117
- Romano D., Matteucci F., Ventura P., D'Antona F., 2001, *A&A*, 374, 646
- Romano D. et al., 2021, *A&A*, 653, A72
- Schwarz G. J. et al., 2011, *ApJS*, 197, 31
- Selvelli P., Gilmozzi R., 2019, *A&A*, 622, A186
- Selvelli P., Molaro P., Izzo L., 2018, *MNRAS*, 481, 2261
- Shore S. N., De Gennaro Aquino I., 2020, *A&A*, 639, L12
- Shore S. N. et al., 2003, *AJ*, 125, 1507
- Siegert T. et al., 2018, *A&A*, 615, A107
- Siegert T., Ghosh S., Mathur K., Spraggon E., Yeddanapudi A., 2021, *A&A*, 650, A187
- Sokolovsky K., Aydi E., Chomiuk L., Kawash A., Strader J., Mukai K., Li K.-L., 2021, *The Astronomer's Telegram*, 14535, 1
- Starrfield S., Truran J. W., Sparks W. M., Arnould M., 1978, *ApJ*, 222, 600
- Starrfield S., Bose M., Iliadis C., Hix W. R., Woodward C. E., Wagner R. M., 2020, *ApJ*, 895, 70
- Taguchi K., Kawabata M., Yamanaka M., Isogai K., 2021, *The Astronomer's Telegram*, 14513, 1
- Tajitsu A., Sadakane K., Naito H., Arai A., Aoki W., 2015, *Nature*, 518, 381
- Tajitsu A., Sadakane K., Naito H., Arai A., Kawakita H., Aoki W., 2016, *ApJ*, 818, 191
- Wallerstein G., Sneden C., 1982, *ApJ*, 255, 577
- Williams R. E., Hamuy M., Phillips M. M., Heathcote S. R., Wells L., Navarrete M., 1991, *ApJ*, 376, 721
- Williams R., Mason E., Della Valle M., Ederoclite A., 2008, *ApJ*, 685, 451

This paper has been typeset from a $\text{T}_{\text{E}}\text{X}/\text{L}^{\text{A}}\text{T}_{\text{E}}\text{X}$ file prepared by the author.